Energy Sharing Mechanism for a Freeform Robotic System - FreeBOT

Guanqi Liang[1,2], Yuxiao Tu[1,2], Lijun Zong[3], Junfeng Chen[2], and Tin Lun Lam[1,2,†]

***Abstract*— Energy sharing in modular self-reconfigurable robots ensures the energy balance of the modules, thus allowing the system to work sustainably. This paper proposes an energy sharing mechanism for a novel modular self-reconfigurable robot that allows free connections among modules, termed as FreeBOT, such that each FreeBOT can share energy with peers through surface contact. Corresponding energy sharing rules are proposed to achieve an energy sharing network structure without invalid components. As alternative choices, several types of networks subjected to the above requirements are provided, which also maximize the number of FreeBOTs joining to share energy. We implement and test the prototype of the energy sharing mechanism on FreeBOT. The experimental results show that the mechanism can effectively achieve energy sharing among FreeBOTs.**

I. Introduction

In recent years, distributed robotic systems have been widely studied and applied [1]–[5]. However, in a distributed robotic system, each robot may be responsible for different tasks and therefore they have different residual energy. If some critical robots run out of energy first, then the robotic system may not be able to complete the task. Energy sharing among robots can effectively enable energy scheduling in a distributed robotic system and ensure sustainable work.

Some studies have been focusing on the methods and applications of energy sharing on distributed robotic systems. Based on the assumption that agents in the system can share energy, many energy scheduling strategies have been proposed [6]–[9]. These studies have all come to a common conclusion that the benefits of energy sharing in distributed robotic systems are enormous. However, these exciting studies are still at the simulation stage and very few have been reported about the implementation of energy sharing in realistic robotic systems. Several distributed robotic systems physically demonstrate energy transfer between two agents [10]–[12], but such mechanism limits energy scheduling efficiency and is not suitable for extension to large-scale robotic systems.

Modular Self-Reconfigurable Robot(MSRR) systems are a special class of distributed robotic systems in which the modules(agents) can physically combine to form a variety of configurations to cope with different task requirements [13]–[20]. Energy depletion of modules will inevitably affect the proper function of the entire modular robotic system. Therefore, it is a challenging topic to combine the onboard energy of each module into one large energy source to power the whole. The vast majority of MSRRs implement docking between modules mainly through fixed-position connectors, and those connectors are easily extended into a switchable real-time energy transfer channel [21]. FreeBOT is a modular self-reconfigurable robot with arbitrary connection points, while the modules can freely connect through a spherical shell and magnets [22]–[24]. However, managing the battery of FreeBOT is difficult due to the coverage of the spherical shell. Before the mechanism proposed in this paper, once the FreeBOT ran out of power, it could not be recharged or restarted unless the shell was disassembled. It is conceivable that there are greater challenges in implementing energy sharing on such a modular self-reconfigurable robotic system that cannot directly manage batteries.

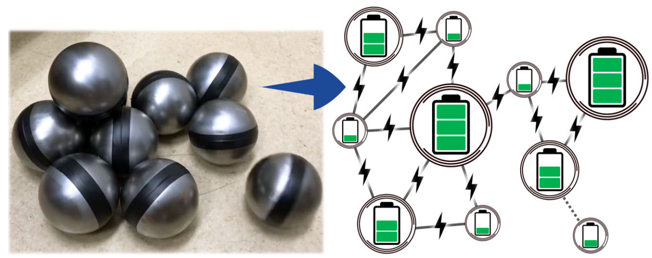

Fig. 1. Energy sharing mechanism for FreeBOT

In this paper, we propose an energy sharing mechanism for FreeBOT that allows each FreeBOT to share energy with peers through surface contact. Corresponding energy sharing rules are proposed to ensure that the formed energy sharing network structure is without invalid components that cause short circuits / open circuits / cycles. As alternative choices, several types of networks subjected to the above requirements are provided, which also maximize the number of FreeBOTs joining to share energy. We implement and test the prototype of the proposed mechanism on FreeBOT, which is the first approach to solve the problem of 3D freeform robot energy sharing. The experimental results show that the mechanism can effectively achieve energy sharing among FreeBOTs.

II. Design

A. Mechanical Design

FreeBOT is a freeform modular self-reconfigurable robotic system that consists of two main parts: an internal driving vehicle equipped with a magnet, and a ferromagnetic spherical shell. The internal magnet in each FreeBOT is able to attract

*This work was supported by the National Natural Science Foundation of China (62073274), and the funding AC01202101103 from the Shenzhen Institute of Artificial Intelligence and Robotics for Society.

[1]School of Science and Engineering, The Chinese University of Hong Kong, Shenzhen, Guangdong, China.

[2]Shenzhen Institute of Artificial Intelligence and Robotics for Society, The Chinese University of Hong Kong, Shenzhen, Guangdong, China.

[3]Institute of Robotics and Intelligent Manufacturing, The Chinese University of Hong Kong, Shenzhen, Guangdong, China.

[†]Corresponding author is Tin Lun Lam `tllam@cuhk.edu.cn`

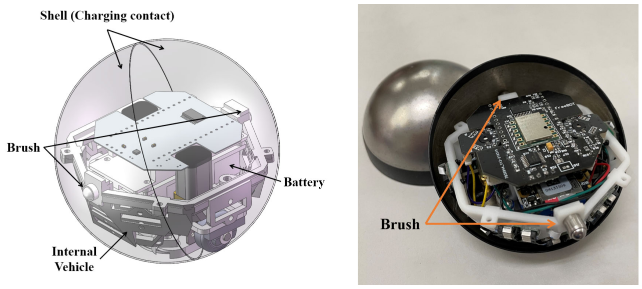

(a) CAD design (b) Prototype

Fig. 2. FreeBOT with energy sharing mechanism

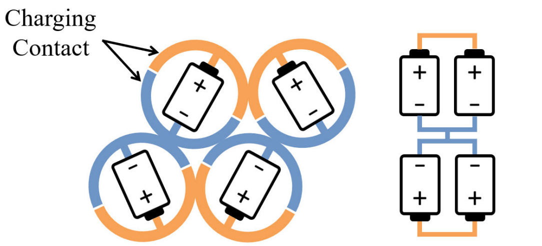

Fig. 3. FreeBOTs form a network through energy sharing mechanism

the entire ferromagnetic shell surface of other FreeBOTs, so each FreeBOT can be connected to any point on other surfaces [22]. The system can be easily rearranged and flexibly transformed into various configurations. However, since the FreeBOT is contained inside the closed shell, it is difficult to operate the internal battery without disassembly, and it is even more challenging to achieve energy sharing among FreeBOTs.

To operate the battery directly from the outside of the FreeBOT, we added a switchable brush mechanism to the internal vehicle that extends the battery port to the outside (as shown in Fig. 2). The brush mechanism is essentially a conductive spring that connects the internal mechanism to the shell in a tight and movable manner. With the proposed mechanism, in any pose of the internal mechanism, the battery port always effectively extends to both hemispheres of the shell. These two conductive hemisphere shells, termed as charging contacts, are not directly connected to each other. Moreover, there is a polarity conversion circuit between the charging contacts and the batteries (see next section), based on which the batteries of multiple FreeBOTs connected in parallel will be adjusted to the same polarity so that their batteries are always connected in parallel with the same polarity. Parallel FreeBOTs are in the same energy sharing subnet and can share energy(as shown in Fig. 3). It is worth mentioning that although FreeBOTs can magnetically connect only one peer, the overlap of charging contacts in the proposed mechanism does not require a magnetic connection; as long as the charging contacts are in contact, it is a valid circuit connection.

B. Circuit Design

The proposed mechanical design ensures that multiple FreeBOTs can be combined to form a physical network through charging contacts. Further, to ensure that the batteries are always connected in parallel with the same polarity

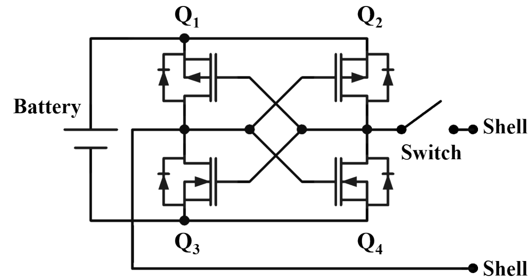

Fig. 4. H-bridge based polarity conversion circuit

within the formed network, a circuit capable of automatically adjusting the polarity is desired. To achieve this, we adopt the H-bridge circuit as the polarity conversion circuit(as shown in Fig. 4). The proposed circuit has two modes:

- **Open-circuit mode.** By default, the robot is in open-circuit mode; it is open between the two charging contacts.
- **Energy sharing mode.** If the robot is in energy sharing mode, its battery can join the energy sharing network through the charging contacts.

FreeBOT is in open-circuit mode by default, so physical contact between FreeBOT shells will not result in battery contact, which is to prevent safety issues caused by accidental contact. In contrast, the energy sharing mode connects the polarity conversion circuit to the charging contacts, and the circuit matches the polarity of the battery with that from the charging contacts. If the voltage from the charging contact is positive, MOSFETs Q_2 and Q_3 will turn on, while Q_1 and Q_4 will turn off. Conversely, if the voltage from the charging contact is negative, MOSFETs Q_1 and Q_4 will turn on, while Q_2 and Q_3 will turn off. Overall, the FreeBOTs in parallel share two charging contacts, and the polarity conversion circuit ensures that their batteries are connected in parallel with the same polarity. The resulting network consists of a series of parallel circuits, termed as energy-sharing subnets, where each FreeBOT will share energy in the subnet it is in. It is worth mentioning that in case of overcurrent, the protection circuit will immediately disconnect the battery from the network; in addition, FreeBOT is powered by an 8.4V lithium battery, the low voltage harmless even when human contact.

III. Energy Sharing Rule

The networks formed by FreeBOTs are random, and there may be safety risks associated with components such as short circuits/cycles in the networks. To ensure the implementation of energy sharing among FreeBOTs, corresponding energy sharing rules are necessary to adjust the network topology so as to transform the random network into a safe and effective energy sharing network.

A. Describing topology with graph theory

Suppose an energy sharing network consists of N robots. The battery of each $robot(i)$ is extended by the proposed mechanical design to two hemispherical shells, termed as $Shell(i)_1$ and $Shell(i)_2$, $(i = 1, 2, ..., n)$. N robots' batteries

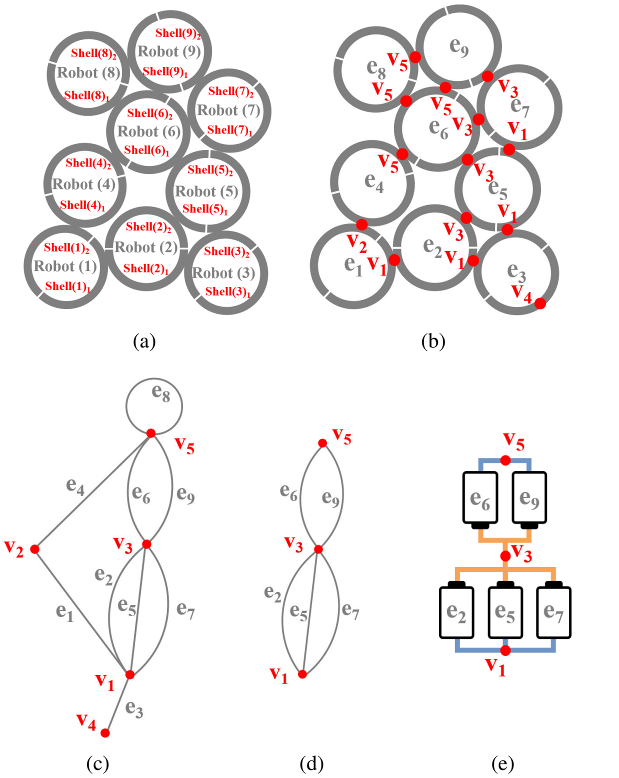

Fig. 5. An energy sharing network example. (a) Network formed by real FreeBOTs; (b) Network topology with contact charging contacts are marked as the same vertex; (c) Undirected graph obtained from network topology; (d) Simplified undirected graph; (e) Resulting energy-sharing network.

are connected through these shells to form an energy sharing network, where the contacted shells will be marked as the same vertex in the energy sharing network. The energy sharing network of robots can be represented by an undirected graph. Let $G =< V, E >$, $E = \{e_1, e_2, ..., e_i, ..., e_m\}$, $V = \{v_1, v_2, ..., v_j, ..., v_n\}$, where edge e_i denotes $robot(i)$, and v_j denotes a vertex connected by one or more charging contacts. Then we use the incidence matrix to represent the connection relationship among the robot batteries. The incidence matrix of G is $M(G) = (m_{ij})_{n\times m}$, where

$$m_{ij} = \begin{cases} 1 & \text{if the } i^{\text{th}} \text{ vertex is a vertex of the } j^{th} \text{ edge} \\ 0 & \text{otherwise} \end{cases} \tag{1}$$

The energy sharing network in Fig. 5 is an example for explaining the related terminology. Following the definition mentioned above, we mark the contacted shells in Fig. 5(a) as the same vertex and then obtain the topology shown in Fig. 5 (b), while Fig. 5 (c) is the corresponding undirected graph. Eq. 2 shows the corresponding incidence matrix M. Both Fig. 5 (c) and Eq. 2 can equivalently represent the energy sharing network in Fig. 5.

$$M = \begin{bmatrix} 1 & 1 & 1 & 0 & 1 & 0 & 1 & 0 & 0 \\ 1 & 0 & 0 & 1 & 0 & 0 & 0 & 0 & 0 \\ 0 & 1 & 0 & 0 & 1 & 1 & 1 & 0 & 1 \\ 0 & 0 & 1 & 0 & 0 & 0 & 0 & 0 & 0 \\ 0 & 0 & 0 & 1 & 0 & 1 & 0 & 1 & 1 \end{bmatrix}. \tag{2}$$

B. *Effective energy sharing network*

The graph theory-based description presents the battery network topology formed directly by real robots. However, these randomly formed network topologies may have short circuits / open circuits / cycles, which may lead to energy loss or even affect the battery lifetime. Therefore, it is necessary to remove these invalid components from the network by putting some robots in open-circuit mode to form an effective energy sharing network.

Since the incidence matrix M equivalently represents the topology of the robot energy sharing network, we can obtain how to reduce it to an effective one from the incidence matrix M. There are three steps to calculate an effective energy sharing network:

Step 1 Detects if there is a cycle in M. If there is, break that cycle by switching some robots in the cycle to open-circuit mode while deleting the corresponding column in the matrix M. Repeat step 1 until there are no loops in M.

Step 2 Search the matrix M column by column. If the sum of a column is not equal to 2, remove that column from M. The corresponding robot switches its mode.

Step 3 Search the matrix M row by row. If the sum of a row is equal to 1, remove that row and related columns from M.

We continue with Fig. 5 (c) to demonstrate how to compute the effective energy sharing network. Following the proposed approach: in step 1, we find that v_1-v_2-v_5-v_3-v_1 is a cycle in M. For the principle of proximity, we break the cycle by breaking e_1, i.e., FreeBOT 1 switches to open-circuit mode as well as e_1 in M is deleted; in step 2, the sum of column e_8 is not 2, indicating that e_8 has a short circuit, so it is deleted; in step 3, the sum of row v_4 is 1, indicating that v_4 has an open circuit, so v_4 and e_3 are deleted; the sum of row v_2 is 1, indicating that v_2 is an open circuit, so v_2 and e_4 are deleted; finally, an effective energy sharing network is obtained, as shown in Fig. 5 (d). In the calculated effective energy sharing network, FreeBOTs 2, 5, and 7 are in the v_1-v_3 subnetwork, while FreeBOTs 6 and 9 are in the v_3-v_5 subnetwork.

IV. Energy Sharing Network Types

The previous section explains the calculations from physics to networks. As alternative choices, this section provides several types of networks that are arranged in such a way as to minimize the number of invalid components such as short circuits/open circuits/cycles, and thus maximize the number of robots joining the energy sharing network.

A. *2D minimum energy sharing network*

In 2D space, a minimum energy sharing network consists of three FreeBOTs (as shown in Fig. 6 (a)). In the 2D minimum energy sharing network, the third FreeBOT acts as an intermediary to connect the other two FreeBOTs to form an energy loop. The following calculation demonstrates the pose constraint of each FreeBOT in the 2D minimum network.

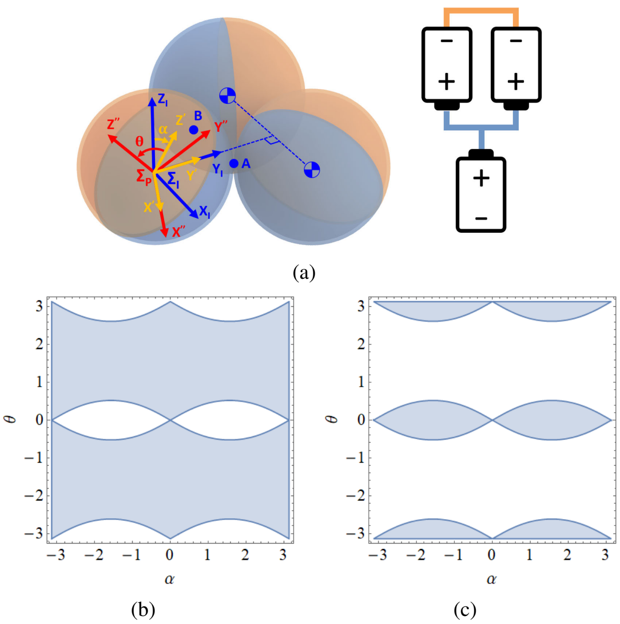

Fig. 6. 2D minimum energy sharing network. (a) Coordinate frames and circuit topology; (b) Pose constrains for robot as intermediary; (c) Pose constrains for robot sharing energy.

In the 2D minimum network, each robot is in contact with the other two ones in the shape of an equilateral triangle, so we first establish the coordinate system as shown in Fig. 6 (a). The radius of the spherical shell is R, then the coordinates of the two contact points in the inertial frame Σ_I are

$$ {}^{I}r_A=\left[\frac{R}{2},\frac{\sqrt{3}R}{2},0\right]^{\mathsf{T}},\ {}^{I}r_B=\left[-\frac{R}{2},\frac{\sqrt{3}R}{2},0\right]^{\mathsf{T}}. \tag{3}$$

The robot's attitude is expressed using $'zyx'$ Euler angle(γ,α,θ). In the body-fixed frame Σ_P, the coordinates of two contact points A and B are

$$ {}^{P}r_A=\begin{bmatrix}\frac{R}{2}c_\alpha\\ \frac{R}{2}s_\alpha s_\theta+\frac{\sqrt{3}R}{2}c_\theta\\ \frac{R}{2}s_\alpha c_\theta-\frac{\sqrt{3}R}{2}s_\theta\end{bmatrix},\ {}^{P}r_B=\begin{bmatrix}-\frac{R}{2}c_\alpha\\ -\frac{R}{2}s_\alpha s_\theta+\frac{\sqrt{3}R}{2}c_\theta\\ -\frac{R}{2}s_\alpha c_\theta-\frac{\sqrt{3}R}{2}s_\theta\end{bmatrix}. \tag{4}$$

In this network type, the intermediary robot contacts the other two robots with one charging contact, while the energy sharing robot contacts the other two robots with two charging contacts, respectively. That is, for the robot acting as an intermediary, the two contacts are located on the same side of the x-y plane of Σ_P, i.e., the z-component of ${}^{P}r_A$ and ${}^{P}r_B$ are of the same sign. For the robot sharing energy, the two contacts are located on different sides of the x-y plane of Σ_P, i.e., the z-component of ${}^{P}r_A$ and ${}^{P}r_B$ are of the opposite sign. Fig. 6 (b) and (c) show the pose range of the robots acting as intermediaries and sharing energy in this network type, respectively.

B. 2D Extended energy sharing network

As an extension of the 2D minimum network, if the FreeBOTs are in contact row by row as shown in Fig. 7 (a), they can all effectively join the energy sharing network. The

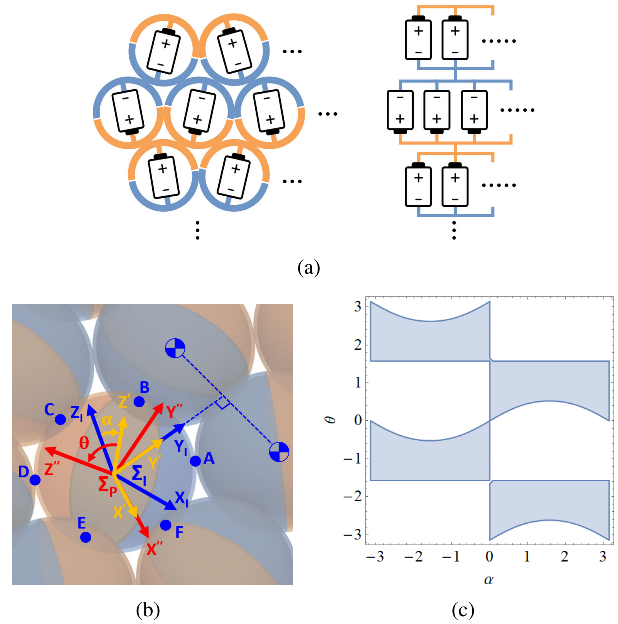

Fig. 7. 2D extended energy sharing network. (a) Circuit topology; (b) Coordinate frames; (c) Pose constrains for robot sharing energy.

resulting extended network does not contain invalid components leading to shorts/open circuits/cycles, etc., and each robot is in energy-sharing mode. The following calculations demonstrate the pose constraints for each robot in the 2D extended network.

We first establish the coordinate system as shown in Fig. 7 (b). Each robot in the 2D extended network is in symmetric contact with the other six robots, and the coordinates of these six contact points in the inertial frame Σ_I are

$$\begin{aligned} &{}^{I}r_A=\left[\frac{R}{2},\frac{\sqrt{3}R}{2},0\right]^{\mathsf{T}}, && {}^{I}r_B=\left[-\frac{R}{2},\frac{\sqrt{3}R}{2},0\right]^{\mathsf{T}},\\ &{}^{I}r_C=[-R,0,0]^{\mathsf{T}}, && {}^{I}r_D=\left[-\frac{R}{2},-\frac{\sqrt{3}R}{2},0\right]^{\mathsf{T}},\\ &{}^{I}r_E=\left[\frac{R}{2},-\frac{\sqrt{3}R}{2},0\right]^{\mathsf{T}}, && {}^{I}r_F=[R,0,0]^{\mathsf{T}}. \end{aligned} \tag{5}$$

Due to the symmetry of the six contacts, the coordinates of three points A, B, and C in the body-fixed frame Σ_P are sufficient to express the pose constraints, which are

$$\begin{aligned} &{}^{P}r_A=\begin{bmatrix}\frac{R}{2}c_\alpha\\ \frac{R}{2}s_\alpha s_\theta+\frac{\sqrt{3}R}{2}c_\theta\\ \frac{R}{2}s_\alpha c_\theta-\frac{\sqrt{3}R}{2}s_\theta\end{bmatrix},\\ &{}^{P}r_B=\begin{bmatrix}-\frac{R}{2}c_\alpha\\ -\frac{R}{2}s_\alpha s_\theta+\frac{\sqrt{3}R}{2}c_\theta\\ -\frac{R}{2}s_\alpha c_\theta-\frac{\sqrt{3}R}{2}s_\theta\end{bmatrix},\ {}^{P}r_C=\begin{bmatrix}-Rc_\alpha\\ -Rs_\alpha s_\theta\\ -Rs_\alpha c_\theta\end{bmatrix}. \end{aligned} \tag{6}$$

In the 2D extended network, one charging contact of each FreeBOT should contact that of the other three FreeBOTs, so that these three contact points are on the same side of the x-y plane of Σ_P, in other words, the z-component of ${}^{P}r_A$, ${}^{P}r_B$, and ${}^{P}r_C$ are of the same sign. Fig. 7 (c) shows the range of α and θ for the robot sharing energy in the 2D extended network.

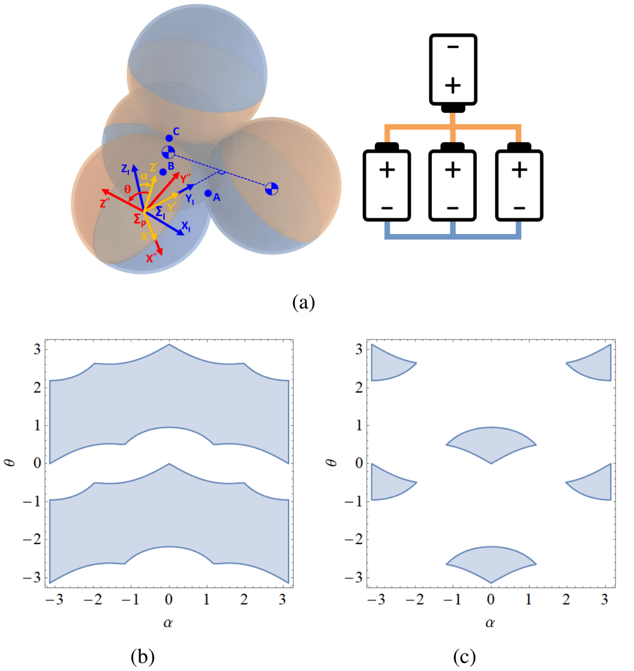

Fig. 8. 3D minimum energy sharing network. (a) Coordinate frames and circuit topology; (b) Pose constrains for robot as intermediary; (c) Pose constrains for robot sharing energy.

C. 3D minimum energy sharing network

In 3D space, a minimum energy sharing network consists of four FreeBOTs (as shown in Fig. 8 (a)). In the 3D minimal energy sharing network, the fourth FreeBOT acts as an intermediary to connect the other three FreeBOTs to form a parallel circuit. The following calculation shows the pose constraint of each FreeBOT in the 3D minimum network, where each robot is in contact with the other three ones in the shape of a tetrahedron, so we first establish the coordinate system as shown in Fig. 8 (a). The coordinates of the three points A, B, and C in the inertial frame Σ_I are

$$\begin{aligned} {}^{I}r_A &= \left[\frac{R}{2}, \frac{\sqrt{3}R}{2}, 0\right]^{\intercal}, \quad {}^{I}r_B = \left[-\frac{R}{2}, \frac{\sqrt{3}R}{2}, 0\right]^{\intercal}, \\ {}^{I}r_C &= \left[0, \frac{\sqrt{3}R}{3}, \frac{\sqrt{6}R}{3}\right]^{\intercal}. \end{aligned} \tag{7}$$

Similarly, the coordinates of A, B, and C in the body-fixed frame Σ_P are

$$\begin{aligned} {}^{P}r_A &= \begin{bmatrix} \frac{R}{2}c_\alpha \\ \frac{R}{2}s_\alpha s_\theta + \frac{\sqrt{3}R}{2}c_\theta \\ \frac{R}{2}s_\alpha c_\theta - \frac{\sqrt{3}R}{2}s_\theta \end{bmatrix}, {}^{P}r_B = \begin{bmatrix} -\frac{R}{2}c_\alpha \\ -\frac{R}{2}s_\alpha s_\theta + \frac{\sqrt{3}R}{2}c_\theta \\ -\frac{R}{2}s_\alpha c_\theta - \frac{\sqrt{3}R}{2}s_\theta \end{bmatrix}, \\ {}^{P}r_C &= \begin{bmatrix} -\frac{\sqrt{6}R}{3}s_\alpha \\ \frac{\sqrt{3}R}{3}c_\theta + \frac{\sqrt{6}R}{3}c_\alpha s_\theta \\ -\frac{\sqrt{3}R}{3}s_\theta + \frac{\sqrt{6}R}{3}c_\alpha c_\theta \end{bmatrix}. \end{aligned} \tag{8}$$

In the 3D minimum network type, the intermediary robot contacts three other robots with one charging contact, i.e., the three contacts are located on the same side of the x-y plane of Σ_P, i.e., the z-component of ${}^{P}r_A$, ${}^{P}r_B$, and ${}^{P}r_C$ are of the same sign. The robot sharing energy has one contact in contact with A and B, while the other charging contact is in contact with C only, that is, A and B are located on the same side of the x-y plane of Σ_P, while C is on the other side. Fig. 8 (b) and (c) show the range of poses of the robots acting as intermediaries and sharing energy in this network type, respectively.

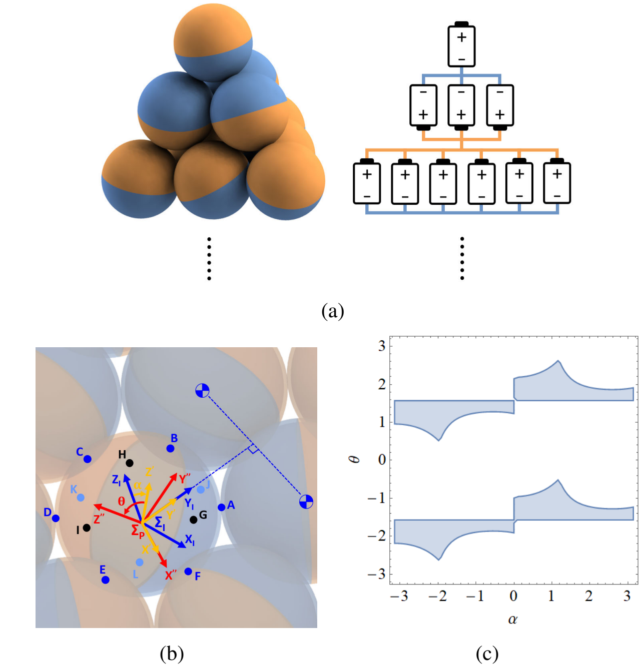

Fig. 9. 3D extended energy sharing network. (a) Circuit topology; (b) Coordinate frames; (c) Pose constrains for robot sharing energy.

D. 3D Extended energy sharing network

As an extension of the 3D minimum network, if the FreeBOTs are arranged layer by layer as shown in Fig. 9 (a), they can all effectively join the energy sharing network. The following calculation shows the pose constraint of each robot in the 3D extended network. We first establish the coordinate system as shown in Fig. 9 (b). Each robot in the 3D extended network is in symmetric contact with the other 12 robots, and the coordinates of these 12 contact points in the inertial frame Σ_I are

$$\begin{aligned} {}^{I}r_A &= \left[\frac{R}{2}, \frac{\sqrt{3}R}{2}, 0\right]^{\intercal}, & {}^{I}r_B &= \left[-\frac{R}{2}, \frac{\sqrt{3}R}{2}, 0\right]^{\intercal}, \\ {}^{I}r_C &= [-R, 0, 0]^{\intercal}, & {}^{I}r_D &= \left[-\frac{R}{2}, -\frac{\sqrt{3}R}{2}, 0\right]^{\intercal}, \\ {}^{I}r_E &= \left[\frac{R}{2}, -\frac{\sqrt{3}R}{2}, 0\right]^{\intercal}, & {}^{I}r_F &= [R, 0, 0]^{\intercal}, \\ {}^{I}r_G &= \left[\frac{R}{2}, \frac{\sqrt{3}R}{6}, \frac{\sqrt{6}R}{3}\right]^{\intercal}, & {}^{I}r_H &= \left[-\frac{R}{2}, \frac{\sqrt{3}R}{6}, \frac{\sqrt{6}R}{3}\right]^{\intercal}, \\ {}^{I}r_I &= \left[0, -\frac{\sqrt{3}R}{3}, \frac{\sqrt{6}R}{3}\right]^{\intercal}, & {}^{I}r_J &= \left[0, \frac{\sqrt{3}R}{3}, -\frac{\sqrt{6}R}{3}\right]^{\intercal}, \\ {}^{I}r_K &= \left[-\frac{R}{2}, -\frac{\sqrt{3}R}{6}, -\frac{\sqrt{6}R}{3}\right]^{\intercal}, & {}^{I}r_L &= \left[\frac{R}{2}, -\frac{\sqrt{3}R}{6}, -\frac{\sqrt{6}R}{3}\right]^{\intercal}. \end{aligned} \tag{9}$$

Considering the symmetry of the contact, the constraint of the pose can be completely described with only six points. Hereby we calculate the coordinates of the points A, B, F, G, H, and J in the body-fixed frame Σ_P:

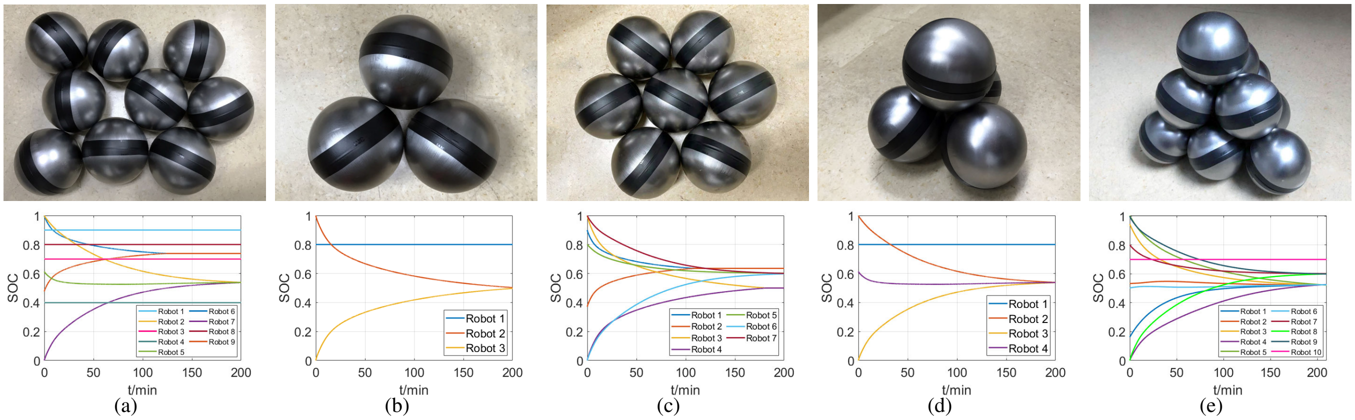

Fig. 10. Experiment and result. (a) the energy sharing network from section III; (b) a 2D minimum energy sharing network example; (c) a 2D extended energy sharing network example; (d) a 3D minimum energy sharing network example; (e) a 3D extended energy sharing network example.

$$
\begin{aligned}
{}^{P}r_A &= \begin{bmatrix} \frac{R}{2}c_\alpha \\ \frac{R}{2}s_\alpha s_\theta + \frac{\sqrt{3}R}{2}c_\theta \\ \frac{R}{2}s_\alpha c_\theta - \frac{\sqrt{3}R}{2}s_\theta \end{bmatrix}, {}^{P}r_B = \begin{bmatrix} -\frac{R}{2}c_\alpha \\ -\frac{R}{2}s_\alpha s_\theta + \frac{\sqrt{3}R}{2}c_\theta \\ -\frac{R}{2}s_\alpha c_\theta - \frac{\sqrt{3}R}{2}s_\theta \end{bmatrix}, \\
{}^{P}r_F &= \begin{bmatrix} Rc_\alpha \\ Rs_\alpha s_\theta \\ Rs_\alpha c_\theta \end{bmatrix}, {}^{P}r_G = \begin{bmatrix} \frac{R}{2}c_\alpha - \frac{\sqrt{6}R}{3}s_\alpha \\ \frac{R}{2}s_\alpha s_\theta + \frac{\sqrt{3}R}{6}c_\theta + \frac{\sqrt{6}R}{3}c_\alpha s_\theta \\ \frac{R}{2}s_\alpha c_\theta - \frac{\sqrt{3}R}{6}s_\theta + \frac{\sqrt{6}R}{3}c_\alpha c_\theta \end{bmatrix}, \\
{}^{P}r_H &= \begin{bmatrix} -\frac{R}{2}c_\alpha - \frac{\sqrt{6}R}{3}s_\alpha \\ -\frac{R}{2}s_\alpha s_\theta + \frac{\sqrt{3}R}{6}c_\theta + \frac{\sqrt{6}R}{3}c_\alpha s_\theta \\ -\frac{R}{2}s_\alpha c_\theta - \frac{\sqrt{3}R}{6}s_\theta + \frac{\sqrt{6}R}{3}c_\alpha c_\theta \end{bmatrix}, \\
{}^{P}r_J &= \begin{bmatrix} \frac{\sqrt{6}R}{3}s_\alpha \\ \frac{\sqrt{3}R}{3}c_\theta - \frac{\sqrt{6}R}{3}c_\alpha s_\theta \\ -\frac{\sqrt{3}R}{3}s_\theta - \frac{\sqrt{6}R}{3}c_\alpha c_\theta \end{bmatrix}.
\end{aligned} \tag{10}
$$

In the 3D extended network, one charging point of each FreeBOT should contact that of the other six FreeBOTs such that these six contact points are on the same side of the x-y plane in the body-fixed frame Σ_P. In other words, the z-components of ${}^{P}r_A$, ${}^{P}r_B$, ${}^{P}r_F$, ${}^{P}r_G$, ${}^{P}r_H$, and ${}^{P}r_J$ are of the same sign. Fig. 9 (c) shows the range of α and θ for the robots in the 3D extended network.

V. Experiment and Results

A. Verification of the energy sharing rule

Fig. 10 (a) shows the verification of the network in Fig. 5. The final state of charge (SoC) of FreeBOTs 2, 5, and 7 converge to about 0.55, while that of FreeBOTs 6 and 9 converge to about 0.75. FreeBOTs 1, 3, 4, and 8 do not join the energy sharing network, so their SoC doesn't change.

B. 2D minimum energy sharing network

Fig. 10 (b) shows a 2D minimum energy sharing network, in which FreeBOT 1 is the intermediary and FreeBOT 2 shares energy with FreeBOT 3. Since FreeBOT 1 serves as an intermediary, its SoC is a constant. FreeBOT 2 keeps charging FreeBOT 3 until the SoC reaches equilibria.

C. 2D extended energy sharing network

Fig. 10 (c) shows a 2D extended energy sharing network consisting of seven FreeBOTs with three subnets. Each FreeBOT shares energy separately in the subnet they belong to, and the three subnets end up with three equilibria.

D. 3D minimum energy sharing network

Fig. 10 (d) shows a 3D minimum energy sharing network where FreeBOT 4 is the intermediary, while FreeBOT 1, 2 and 3 share energy. Thus, the SoC of FreeBOT 1 is a constant, while FreeBOT 2, 3 and 4 keep sharing energy until all their SoCs reach about 0.52.

E. 3D extended energy sharing network

Fig. 10 (e) shows a 3D extended energy sharing network consisting of ten FreeBOTs with three subnets. FreeBOT 1 is an intermediary, so its SoC is a constant. The other FreeBOTs are divided into two subnets, and the two subnets end up with two equilibria.

VI. Conclusions and Future Work

In this paper, we propose an energy sharing mechanism for FreeBOT that allows each robot to share energy with peers through surface contact. This paper proposed, analyzed, and validated the first approach to solve the problem of 3D freeform robot energy sharing. However, some aspects can be further improved in the future:

1) The proposed energy sharing solution is only applicable to static configurations, and cannot achieve energy sharing among modules in dynamic configurations.
2) The proposed rules can remove unsafe and invalid components from the network, but this requires centralized global information. Currently, the information is obtained mainly through external sensors.

Overall, although this work has some limitations, it is the only solution for FreeBOT energy sharing so far. We will further investigate better solutions in the future to solve the above limitations, expecting to achieve an energy sharing FreeBOT system that is free from external sensors and can work sustainably

REFERENCES

[1] M. Corah, C. O'Meadhra, K. Goel, and N. Michael, "Communication-efficient planning and mapping for multi-robot exploration in large environments," *IEEE Robotics and Automation Letters*, vol. 4, no. 2, pp. 1715–1721, 2019.

[2] X. Zhou, J. Zhu, H. Zhou, C. Xu, and F. Gao, "Ego-swarm: A fully autonomous and decentralized quadrotor swarm system in cluttered environments," in *2021 IEEE International Conference on Robotics and Automation (ICRA)*. IEEE, 2021, pp. 4101–4107.

[3] N. Han, J. Luo, and L. Zong, "Cooperative game method for on-orbit substructure transportation using modular robots," *IEEE Transactions on Aerospace and Electronic Systems*, 2021.

[4] X. Guo, J. Hu, J. Chen, F. Deng, and T. L. Lam, "Semantic histogram based graph matching for real-time multi-robot global localization in large scale environment," *IEEE Robotics and Automation Letters*, vol. 6, no. 4, pp. 8349–8356, 2021.

[5] M. Li, G. Liang, H. Luo, H. Qian, and T. L. Lam, "Robot-to-robot relative pose estimation based on semidefinite relaxation optimization," in *2020 IEEE/RSJ International Conference on Intelligent Robots and Systems (IROS)*. IEEE, pp. 4491–4498.

[6] T. D. Ngo, H. Raposo, and H. Schioler, "Potentially distributable energy: Towards energy autonomy in large population of mobile robots," in *2007 International Symposium on Computational Intelligence in Robotics and Automation*. IEEE, 2007, pp. 206–211.

[7] N. Kamra, T. S. Kumar, and N. Ayanian, "Combinatorial problems in multirobot battery exchange systems," *IEEE Transactions on Automation Science and Engineering*, vol. 15, no. 2, pp. 852–862, 2017.

[8] T. Mina and B.-C. Min, "Penguin huddling-inspired energy sharing and formation movement in multi-robot systems," in *2018 IEEE International Symposium on Safety, Security, and Rescue Robotics (SSRR)*. IEEE, 2018, pp. 1–8.

[9] D. Niyato, P. Wang, D. I. Kim, W. Saad, and Z. Han, "Mobile energy sharing networks: Performance analysis and optimization," *IEEE Transactions on Vehicular Technology*, vol. 65, no. 5, pp. 3519–3535, 2015.

[10] N. Mathew, S. L. Smith, and S. L. Waslander, "Multirobot rendezvous planning for recharging in persistent tasks," *IEEE Transactions on Robotics*, vol. 31, no. 1, pp. 128–142, 2015.

[11] A. Couture-Beil and R. T. Vaughan, "Adaptive mobile charging stations for multi-robot systems," in *2009 IEEE/RSJ international conference on intelligent robots and systems*. IEEE, 2009, pp. 1363–1368.

[12] A. Drenner, M. Janssen, and N. Papanikolopoulos, "Coordinating recharging of large scale robotic teams," in *2009 IEEE/RSJ International Conference on Intelligent Robots and Systems*. IEEE, 2009, pp. 1357–1362.

[13] C. Wright, A. Buchan, B. Brown, J. Geist, M. Schwerin, D. Rollinson, M. Tesch, and H. Choset, "Design and architecture of the unified modular snake robot," in *2012 IEEE International Conference on Robotics and Automation*. IEEE, 2012, pp. 4347–4354.

[14] T. Tosun, J. Davey, C. Liu, and M. Yim, "Design and characterization of the ep-face connector," in *2016 IEEE/RSJ International Conference on Intelligent Robots and Systems (IROS)*. IEEE, 2016, pp. 45–51.

[15] Y. Tu, G. Liang, and T. L. Lam, "FreeSN: A freeform strut-node structured modular self-reconfigurable robot - design and implementation," in *2022 IEEE International Conference on Robotics and Automation (ICRA)*. IEEE, 2022.

[16] J. W. Romanishin, K. Gilpin, S. Claici, and D. Rus, "3d m-blocks: Self-reconfiguring robots capable of locomotion via pivoting in three dimensions," in *2015 IEEE International Conference on Robotics and Automation (ICRA)*. IEEE, 2015, pp. 1925–1932.

[17] H. Luo, M. Li, G. Liang, H. Qian, and T. L. Lam, "An obstacle-crossing strategy based on the fast self-reconfiguration for modular sphere robots," in *2020 IEEE/RSJ International Conference on Intelligent Robots and Systems*. IEEE, 2020, pp. 3296–3303.

[18] J. Neubert, A. Rost, and H. Lipson, "Self-soldering connectors for modular robots," *IEEE Transactions on Robotics*, vol. 30, no. 6, pp. 1344–1357, 2014.

[19] A. Spröwitz, R. Moeckel, M. Vespignani, S. Bonardi, and A. J. Ijspeert, "Roombots: A hardware perspective on 3d self-reconfiguration and locomotion with a homogeneous modular robot," *Robotics and Autonomous Systems*, vol. 62, no. 7, pp. 1016–1033, 2014.

[20] P. Swissler and M. Rubenstein, "Fireant3d: a 3d self-climbing robot towards non-latticed robotic self-assembly," in *2020 IEEE/RSJ International Conference on Intelligent Robots and Systems*. IEEE, 2020.

[21] K. Holdcroft, C. H. Belke, S. Bennani, and J. Paik, "3pac: A plug-and-play system for distributed power sharing and communication in modular robots," *IEEE/ASME Transactions on Mechatronics*, 2021.

[22] G. Liang, H. Luo, M. Li, H. Qian, and T. L. Lam, "FreeBOT: A freeform modular self-reconfigurable robot with arbitrary connection point-design and implementation," in *2020 IEEE/RSJ International Conference on Intelligent Robots and Systems*. IEEE, 2020, pp. 988–995.

[23] T. L. Lam and G. Liang, "Self-reconfigurable robot module and self-reconfigurable robot," Jul. 8 2021, US Patent App. 17/134,066.

[24] Y. Tu, G. Liang, and T. L. Lam, "Graph convolutional network based configuration detection for freeform modular robot using magnetic sensor array," in *2021 IEEE International Conference on Robotics and Automation (ICRA)*. IEEE, 2021, pp. 4252–4258.